General Exam Research Presentation Extended Abstract

Daniel Ruth

October 19, 2018

The interaction between Earth's atmosphere and its oceans plays a key role in marine biological processes, the global carbon cycle, and local weather phenomena. Turbulent mixing at the water's surface, induced by surface-level winds, greatly increases the rate at which mass, momentum and heat exchanges can take place relative to quiescent conditions, in which molecular diffusion dominates. Additionally, when the wind is strong enough, breaking waves at the surface will entrain air bubbles into the water, greatly enhancing exchanges between the oceans and the atmosphere [3, 1]. Turbulence in the upper layer of the ocean can break these bubbles apart and slow their rise to the surface, increasing the time and surface area available for their gases to diffuse to the water. A key step to improving this gas transfer parameterization is then relating the behavior of the bubbles to the turbulence characteristics of their surroundings. Understanding bubble statistics will also lead to more accurate boundary conditions for models of the spray produced as a bubble reaches the surface and bursts, which is an important mechanism in cloud formation.

The breakup criteria for bubbles in turbulence is described by the Weber number, which characterizes the ratio of the turbulence's dynamic stresses on the bubble to the restoring force of surface tension. This leads to $\mathrm{We} = \rho \overline{\delta u^2(d)} d/\sigma$, where $\overline{\delta u^2(d)}$ is a typical squared velocity difference over the distance of the bubble diameter. If the turbulence is homogeneous and isotropic and d falls within its inertial subrange, Komogorov's description of turbulence leads to $\overline{\delta u^2(d)} = 2(\epsilon d)^{2/3}$, where ϵ is the dissipation rate of the turbulence. Neglecting the order-1 constant, this leads to $\mathrm{We} = \rho \epsilon^{2/3} d^{5/3}/\sigma$ [4]. One approach to modeling the breakup probability holds that breakup will occur beyond some order-1 critical Weber number representing a balance between inertial and surface tension forces [4]. However, since the turbulence is described by distributions of probabilities for velocity differences, a full description of breakup likelihood is more nuanced [6]. Additionally, this force-balance approach does not describe the distribution of child bubble sizes which result from breakup events. Experiments can be used to understand the breakup statistics as a more detailed function of the various turbulence and bubble properties [6].

I will detail the experimental capabilities I have developed over the past year, which will be used to probe bubble phenomena. The primary apparatus consists of a water tank in which water jet pumps are arranged at the corners of a $\mathcal{O}(10\,\mathrm{cm})$ cube, point sources of momentum directed towards the cube center. When turned on, these pumps induce a turbulent flowfield at the cube center, and the symmetry of the setup yields a small mean flow. The use of jet pumps for such an apparatus follows the work of Variano and Cowen [7], but scales down the size and adopts the geometry of Hwang and Eaton [5] in order to incerase the dissipation rate. Particle image velocimetry (PIV) is employed to characterize the turbulence, and dissipation rates on the order of $10^3\,\mathrm{cm}^2/\mathrm{s}^3$ to $10^4\,\mathrm{cm}^2/\mathrm{s}^3$ are achieved. High-speed cameras are used to track the bubbles in this turbulence region, from which quantities such as velocity and size distributions and contour shapes are extracted. Optical access from multiple angles enables the three-dimensional tracking of bubbles with a two-camera stereo vision setup.

Finally, I will discuss progress I have made with this setup in characterizing the dynamics of turbulence-induced bubble pinch-off. Pinch-off of gas bubbles from needles in quiescent liquids is a much-studied and well-understood phenomena. Up until the final portion of the process, the pinch-off is well-described by an inertial model in which the inertia of the gas, the surface tension at the gas-liquid interface, and the fluid viscosities are negligible. Such a model leads to a self-similar solution for the neck collapse, in which the minimum neck width d_0 is related to the time remaining until pinch-off τ as $d_0 \sim \tau^\alpha$, with $\alpha \approx 0.5$ [2].

Preliminary data shows that turbulence-induced breakup of free bubbles does not always follow this $\alpha \approx 0.5$ power law for significant portions of the pinch-off process. Instead, a wide distribution of power law exponents is observed over many realizations of free bubbles breaking apart or pinching off from needles

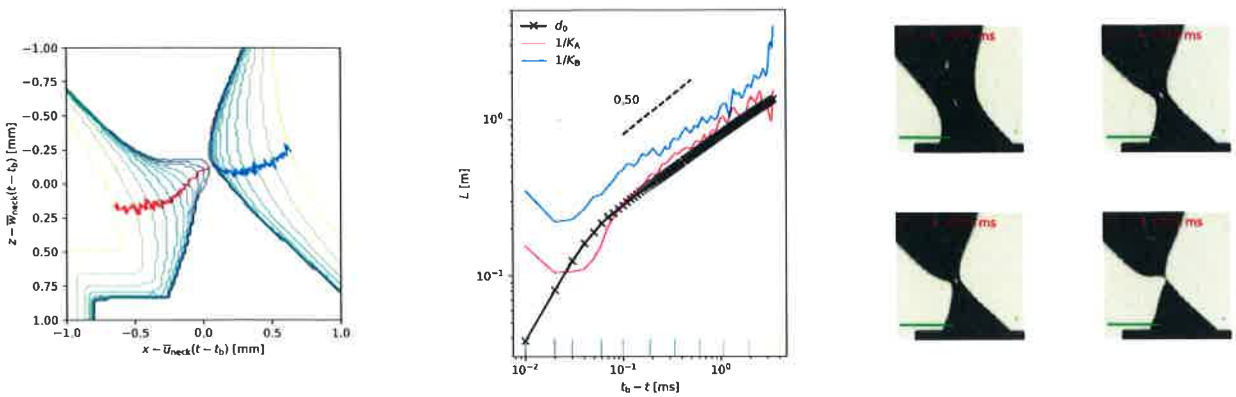

Figure 1: Illustration of one asymmetric case of turbulent needle pinch-off. The image on the left shows the contour of the detaching bubble at various moments in time, corresponding to the times at which notches are placed at the bottom of the plot in the center. The red and blue curves show the trajectories taken by the two sides of the neck. In the middle, the neck size d_0 is plotted against time until breakup in black, and the radii of curvature of either side of the neck are shown in red and blue. Finally on the right, four snapshots of the neck region at various times before pinch-off are shown. The green bar represents 1 mm.

in a turbulent background. We see that while the neck collapse for bubbles sent from needles without turbulence behaves as expected, the introduction of turbulence clearly complicates the process. Through image processing techniques, I relate differences in the behavior of the two sides of the neck to the observed behavior of the $d_0(\tau)$ curve.

In many turbulent cases, the collapse is not axisymmetric, as the two sides of the collapsing neck move with different velocities and curvatures. This asymmetry often persists through the entirety of the breakup, or becomes more pronounced during the final stages. One such case is illustrated in Figure 1. The red-colored side of the collapsing neck is at a consistently higher curvature. At around 100 µs prior to pinch-off, the collapse accelerates (visible as the change of slope in the middle plot of the neck size over time). This is associated with the asymmetry becoming more pronounced (the appearance of the kink) in the purple bubble contour curves shown on the left plot and in the final image shown on the right.

In other cases, the final moment of pinch-off is delayed as the neck collapse rapidly slows. Future work will involve further characterizing these phenomena using a two-camera stereo vision system and identifying the physical mechanism behind the changes in collapse behavior. Finally, the physics controlling bubble breakup will be related to the distribution of child bubble sizes yielded by the turbulent breakup of bubbles of a given size.

[1] L. Deike, W. K. Melville, and S. Popinet. In: *Journal of Fluid Mechanics* 801 (2016), pp. 91–129. ISSN: 0022-1120. DOI: 10.1017/jfm.2016.372.

[2] J. Eggers et al. In: *Physical Review Letters* 98.9 (2007), pp. 1–4. ISSN: 00319007. DOI: 10.1103/PhysRevLett.98.094502. arXiv: 0610139 [physics].

[3] Christoph S Garbe et al. 2014. ISBN: 978-3-642-25642-4. DOI: 10.1007/978-3-642-25643-1.

[4] J. O. Hinze. In: *AIChE Journal* 1.3 (1955), pp. 289–295. ISSN: 15475905. DOI: 10.1002/aic.690010303. arXiv: arXiv:1011.1669v3.

[5] W. Hwang and J. K. Eaton. In: *Experiments in Fluids* 36.3 (2004), pp. 444–454. ISSN: 07234864. DOI: 10.1007/s00348-003-0742-6.

[6] F. Risso and J. Fabre. In: *Journal of Fluid Mechanics* 372.1998 (1998), pp. 323–355. ISSN: 00221120. DOI: 10.1017/S0022112098002705.

[7] Evan Variano and Edwin Cowen. In: *Journal of Fluid Mechanics* 604 (2008), pp. 1–32. ISSN: 0022-1120. DOI: 10.1017/S0022112008000645.